

1 **The impact of allometry on vomer shape and its implications for the taxonomy and**
2 **cranial kinesis of crown-group birds**

3
4 Olivia Plateau^{1*}, Christian Foth¹

5 ¹Department of Geosciences, University of Fribourg, Chemin du Musée 6, CH-1700
6 Fribourg, Switzerland

7 *e-mail: olivia.plateau@unifr.ch

8
9 O.P. (ORCID: 0000-0002-8321-2687)

10 C.F. (ORCID: 0000-0002-9410-4569)

11
12 **Abstract**

13 Crown birds are subdivided into two main groups, Palaeognathae and Neognathae, that can
14 be distinguished, **among other means**, by the organization of the bones in their pterygoid-
15 palatine complex (PPC). Shape **variation of the vomer**, which is the most anterior part of the
16 PPC, was **recently analysed with help of** geometric morphometrics to discover morphological
17 differences between palaeognath and neognath birds. Based on this study, the vomer was
18 identified as sufficient to distinguish the two main groups (and even **some** inclusive neognath
19 groups) and their cranial kinetic system. As there are notable size differences between the
20 skulls of **Palaeognathae** and **Neognathae**, we here investigate the impact of allometry on
21 vomeral shape and its implication for taxonomic classification by re-analysing the data of the
22 previous study. Different types of multivariate statistical analyses reveal that taxonomic
23 identification based on vomeral shape is strongly impaired by allometry, as the error of
24 correct identification is high when shape data is corrected for size. This finding is **evidenced**
25 by a great overlap between palaeognath and neognath subclades in morphospace. **Correct**

26 **taxonomic identification is further impeded** by the convergent presence of a flattened vomeral
27 morphotype in multiple neognath subclades. As the evolution of cranial kinesis has been
28 linked to vomeral shape in the original study, **the correlation** between shape and size of the
29 vomer across different bird groups found in the present study questions this conclusion. In
30 fact, cranial kinesis in crown birds results from the loss of the jugal-postorbital bar in the
31 temporal region and ectopterygoid in the PPC and the combination of a mobilized quadrate-
32 zygomatic arch complex and a flexible PPC. Therefore, we can conclude that **vomer shape**
33 itself is not a suitable proxy for exploring the evolution of cranial kinesis in crown birds and
34 their ancestors. **In contrast, the evolution of cranial kinesis needs to be viewed in context of**
35 **the braincase, quadrate-zygomatic arch and the whole pterygoid-palatine complex.**

36

37 **Introduction**

38 The pterygoid-palatine complex (PPC) of crown birds is mainly formed by five bones: the
39 unpaired vomer that results from the fusion of the originally paired vomer **elements**, and the
40 paired pterygoids and palatines. **The general morphology of the PPC** was first studied by
41 Huxley (1867), who distinguished the clade Palaeognathae from all other birds on the basis of
42 palatal morphology. Although the PPC of **Palaeognathae** is quite variable (McDowell 1948),
43 it is characterized by a large vomer that is only partly fused. The pterygoids and palatines are
44 highly connected, forming a rigid unit that articulates with the braincase via well-developed
45 basiptyergoid processes, while a contact with the parasphenoid is not present (see Bellairs &
46 Jenkin 1960; Zusi 1993; Gussekloo et al. 2001, Mayr 2017; Fig. 1A). In contrast, neognath
47 birds possess a movable joint between pterygoid and palatine, which plays an important role
48 in the kinematic movement of the upper jaw. Here, the pterygoid articulates with the
49 parasphenoid, while the basiptyergoid processes are often reduced. The vomer is highly
50 variable in size and shape and often has no connection with the upper jaw beyond an

51 association with the nasal septum and the palatine. In some neognaths, the vomer is greatly
52 reduced or even absent (see Bellairs & Jenkin 1960; Bock 1964; Zusi 1993; Mayr 2017, Fig.
53 1A).

54 In a recent paper, Hu et al. (2019) investigated palate evolution in crown birds and
55 their stem, focusing on the morphology of the vomer. Using 3D geometric morphometrics,
56 the study found that the vomeral shape of neognaths is clearly distinguishable from
57 *Palaeognathae*, in that the latter group has a stronger similarity with their non-avian
58 ancestors. Linking vomer shape with the kinetic abilities of the skull, the authors concluded
59 that cranial kinesis represents an innovation of Neognathae. Furthermore, the authors
60 concluded that vomeral morphology allows for a taxonomic differentiation between the major
61 groups of *Neognathae*, namely Aequorlitorinithes, *Galloanserae*, Gruiformes, and Inopinaves.
62 However, according to their PCA results, all groups strongly overlap each other within PC1,
63 while a taxonomic differentiation is only noticeable within PC2 (other principal components
64 are not shown). Taking the great size variation of the vomer of neognath birds into account
65 (Zusi 1993), we wonder if the reported taxonomic differentiation between palaeognaths and
66 the neognath subclades could alternatively be related to allometry, i.e. the dependence of
67 shape on size (Klingenberg 1998), rather than pure shape variation. In order to test this
68 hypothesis, we re-analysed the dataset of Hu et al. (2019), comparing allometric shape data
69 with non-allometric residuals, and re-evaluating the role of the vomer in the evolution of
70 cranial kinesis in crown birds.

71

72 **Materials and Methods**

73 The published 3D models and landmarks data of 41 specimens including 36 species were
74 downloaded from Hu et al. 2019 (<https://doi.org/10.6084/m9.figshare.7769279.v2>). This
75 dataset contains five extinct species (two stem line representatives: the troodontid

76 *Sinovenator changii*, the Avialae *Sapeornis chaoyangensis*; and three fossil palaeognath
77 crown birds from the clade Dinornithiformes: *Pachyornis australis*, *Megalapteryx didinus*
78 and *Diornis robustus*), five extant Paleognathae and 27 extant Neognathae representing the
79 two major clades of crown birds.

80 The original **landmark data** (Dataset A) is composed of five anatomical landmarks and
81 43 semi-landmarks (see Hu et al. 2019). The landmark data were imported into the software
82 *R v.3.5.2* (R Core Team, 2018). Using the *plotAllSpecimens* function of *Geomorph v.3.2.1*
83 (Adams et al. 2013) in *R*, we notice great variability for each anatomical landmark, resulting
84 from two main shapes of the vomer. The majority of bird possesses a fused vomer that is
85 bilaterally symmetric and roof-shaped in transection, with a horizontal orientation within the
86 pterygoid-palatine complex (Fig. 1B). In contrast, some members of Aequorlornithes (e.g.,
87 *Podiceps nigricollis*, and *Podilymbus podiceps*), **Galloanserae** (e.g., *Anas crecca*, *Anseranas*
88 *semipalmata*, and *Cairina moschata*) and Inopinaves (e.g., *Aquila audax*, *Falco cenchroides*,
89 and *Haliastur sphenurus*) possess a fused vomer that is completely mediolaterally flattened in
90 transection and vertically orientated within the pterygoid-palatine complex (Fig. 1B).
91 Therefore, we created a second dataset (Dataset B), where species with this latter, flat vomer
92 morphology were excluded. Furthermore, the palaeognath birds *Struthio camelus* and
93 *Dromaieus novaehollandiae* of the original Dataset A were represented by both juvenile and
94 adult specimens. Because ontogenetic variation could, however, potentially affect size and
95 position of the palaeognath morphospace, we removed the juvenile and subadult specimens
96 of *Struthio camelus* and *Dromaieus novaehollandiae* in order to reran the analysis just with
97 adult semaphoronts (Dataset C). Finally, we created a fourth dataset, where both
98 juvenile/subadult specimens and species with flat vomers were removed from the sample
99 (Dataset D).

100 For superposition of the 3D landmark data, we followed Hu et al. (2019) by
101 performing a *Generalized Procrustes Analysis* (GPA). The GPA was done with the help of
102 the *gpagen* function in *Geomorph*. Afterward, we performed a *principal component analysis*
103 (PCA) in order to visualize the shape variability of the vomer and the variance of
104 morphospace for two groupings: (1) Paleognathae versus Neognathae and (2) Paleognathae,
105 Inopinaves, Galloanserae, Gruiformes and Aequorlitorithes. This was done with the
106 *plotTangentSpace* function from *Geomorph*.

107 Because the vomer showed great variation in centroid size after superimposition,
108 ranging from 14.60 (*Manorina melanocephala*) to 168.32 (*Dromaius novehollandia*), we
109 tested if there is a significant correlation between Procrustes coordinates and log-transformed
110 centroid size (Goodall 1991) using the function *procD.lm* in *Geomorph*. This function
111 performs a multivariate regression between the shape and size with a permutation of 10,000
112 iterations. A significant relationship between both parameters indicates that the superimposed
113 shape still contains an allometric signal. Based on this correlation we estimated non-
114 allometric residuals of the Procrustes coordinates and repeated the PCA. In addition, we
115 tested each of the first eleven PCs that together describe more than 95 of total variation for
116 allometric signals.

117 A set of 1,000 relaxed-clock molecular trees, which follow the topology of Hackett et
118 al. (2008) and summarize the range of uncertainties in terms of time calibration of ancestral
119 nodes, were downloaded from birdtree (<http://birdtree.org>) (Jetz et al. 2012, 2014) including
120 all extant bird species in the dataset (Supplementary Data S1). Due to uncertainties in the
121 taxonomic identification of *Aquila sp.*, this specimen was removed from the sample as we
122 could not include it in the phylogeny. Because the specimen occupies almost the same
123 position as *Aquilla audax*, we consider this deletion to have a negligible effect on the
124 outcome of the analyses. Furthermore, the species *Sterna bergii* and *Grus rubicunda* used in

125 the analysis from Hu et al. (2019) are junior synonyms of *Thalasseus bergii* (Bridge et al.
126 2005) and *Antigone rubicunda* (Krajewski et al. 2010). Using the function *consensus.edges* in
127 the R package *phytools* v.0.7-20, we computed a temporal consensus. The extinct
128 dinornithiform species were placed as sister-group to Tinamidae following Mitchell et al.
129 (2014). Because of their recent extinction (Holdaway & Jacomb 2000; Turvey & Holdaway
130 2005), the age was set to zero, similar to the other crown birds. The stem line representatives
131 *Sinovenator changii* and *Sapeornis chaoyangensis* were added following the time-calibrated
132 phylogeny of Rauhut et al. (2019). Because of the presence of juvenile specimens in dataset
133 A and B, we added the juvenile specimens by splitting OTU (operational taxonomic unit) of
134 *Struthio camelus* and *Dromaieus novehollandia* into a polytomy with each sub-OTU having a
135 branch length of one year (this value had to be standardized, as *pFDA* requires an isometric
136 tree). The impact of phylogeny on shape and centroid size (log-transformed) was tested using
137 the function *physignal* in *Geomorph*. Based on *K*-statistics, this method evaluates the impact
138 of phylogeny on a multivariate dataset relative to what is expected, if evolution is simulated
139 under a Brownian motion model (Blomberg et al. 2003).

140 To explore the size of the single morphospaces of each taxon, we computed the
141 morphological disparity using *morphol.disparity* in *Geomorph*. This analysis uses the
142 Procrustes variance as disparity metric, which is the sum of all diagonal elements of a group
143 covariance matrix divided by the number of observations within the group (Zelditch et al.
144 2012). Statistical comparisons of group sizes were executed with help of a permutation test
145 with 999 iterations. To test for potential overlap in morphospace of vomer shapes in different
146 clades of crown bird (see grouping 1 and 2) and their relation to the stem line representatives
147 *Sinovenator changii* and *Sapeornis chaoyangensis*, we applied three different multivariate
148 statistical methods, using the first eleven PCs as input data. We first applied a nonparametric
149 multivariate analysis of variance (*perMANOVA*). This method evaluates the potential

150 overlapping of groups in morphospace by testing the significance of their distribution on the
151 basis of permutation (10,000 replications) and Euclidean distance (as one of several possible
152 distance measures), not requiring normal distribution of the data (Anderson, 2001; Hammer
153 & Harper, 2006). The spatial relationship of groups relative to each other is expressed by an
154 F value and p value. For the five-group comparison, the p values were Bonferroni-corrected
155 by multiplying the value with the number of comparisons. Next, we ran a discriminant
156 analysis (DA), which reduces a multivariate data set to a **smaller set of** dimensions by
157 maximizing the separation between two or more groups using Mahalanobis distances. This
158 distance measure is estimated from the pooled within-group covariance matrix, resulting in a
159 linear discriminant classifier and an estimated group assignment for each species. The results
160 were cross-validated using Jackknife resampling (Hammer & Harper, 2006; Hammer 2020).
161 Both multivariate tests were done with the program *PAST v.4.03* (Hammer et al. 2001).
162 Finally, we performed a phylogenetic flexible discriminant analysis ($pFDA$) (Schmitz &
163 Motani, 2011; Motani & Schmitz, 2011) in *R*. This method removes the phylogenetic bias
164 from the categorical variables before the actual discriminant analysis is undertaken by
165 estimating Pagel's lambda, which tests how the grouping correlates with phylogeny. This was
166 done for all allometric and non-allometric datasets.

167 The error of correct identification from the resulting confusion matrices was
168 compared between allometric and non-allometric data. For these comparisons, we used non-
169 parametric *Mann-Whitney U* and *Kruskal-Wallis* tests, which both estimates, whether or not
170 two univariate samples were taken from populations with equal medians, being more robust
171 against small sample sizes and data without normal distribution **than parametric tests**
172 (Hammer & Harper 2006). Both tests were **carried out** with *PAST*.

173 Finally, we applied an ordinary least square regression analysis to **19 species** test the
174 correlation between log-transformed vomer **size** and the skull size using a log-transformed

175 box volume (Height x Width x Length). The measurements of the skull box volume were
176 taken from skullsite (<https://skullsite.com>).

177

178 **Results**

179 Based on the *PCA* of the original dataset, the first two PCs explain over 52% (Fig. 2A) of
180 total shape variation (PC1: 27.5%; PC2:25.1%). The morphospace of *Palaeognathae* and
181 *Neognathae* is almost equal in size. Taking the small sample size of *Palaeognathae* into
182 account, the size of their morphospace indicates *relatively* great shape variation. *This is*
183 *supported by the Procrustes variances, which indicates a larger shape disparity in*
184 *Palaeognathae*. Both *Palaeognathae* and *Neognathae* show a strong overlap along PC1 and a
185 partial overlap along PC2. When comparing neognath subclades, *Aequorlornithes* show
186 strong overlap along both PCs with the palaeognath morphospace. *Gruiformes* lie in the
187 overlapping area of both groups. The morphospace of *Inopinaves* and *Galloanserae* overlap
188 with each other *on* both axes, but are separated from *Palaeognathae*, *Aequorlornithes* and
189 *Gruiformes* along PC2. *Within Neognathae, Galloanserae have the largest shape disparity,*
190 *becoming successively smaller in Inopinaves, Aequorlornithes and Gruiformes*
191 *(Supplementary Data S2; S3: Fig. S1; S4: Table S1).*

192 Allometry summarizes about 6.4% of total shape variation. Using non-allometric
193 residuals PC1 explains 29.3% and PC2 22.9% (Fig 2.B). While the general distribution of the
194 single bird clades does not change along PC1, the groups are less separated along PC2, which
195 contains the major allometric signal within the principal components (slope: -0.523; R^2 :
196 0.185; p : 0.005; predicted variation: 19.5%), which is 4.9% of total shape variation in the
197 original dataset. Here, the palaeognath morphospace overlaps fully with *Aequorlornithes*
198 and *Gruiformes*, partly with *Inopinaves* and marginally with *Galloanserae*. For the three other
199 datasets, we observe more or less similar general trends before and after size correction,

200 although the single morphospaces are partly shrunk. In all cases, the two stem line
201 representatives *Sinovenator changii* and *Sapeornis chaoyangensis* lie within the marginal
202 area of the palaeognaths/aequorlitornithines morphospace. Here, vomer morphology of the
203 troodontid *Sinovenator changii* is more bird-like than that of the avialian *Sapeornis*
204 *chaoyangensis*. The exclusion of the allometric shape variation has only a minor impact on
205 disparity. Thus, all disparity trends found in the original dataset persist in the non-allometric
206 datasets (Supplementary Data S2; S3: Fig. S1; S4: Table S1).

207 As previously detected by Hu et al. (2019), vomer shape is impacted by phylogeny.
208 Neither the modification of the sampling nor the exclusion of allometry changes this
209 relationship. In contrast, log centroid size does not contain a phylogenetic signal
210 (Supplementary Data S4: Table S2).

211 In all studied datasets, the *perMANOVA* found a significant separation between
212 palaeognath and neognath birds, showing no impact of allometry. For the five-group
213 comparison of the original dataset (A), the overall results still indicate significant separation
214 between clades for both allometric and non-allometric data. However, group-by-group
215 comparison of allometric data indicates an overlap in morphospace of *Gruiformes* with
216 *Aequorlitornithes*, *Inopinaves*, *Galloanserae* and *Palaeognathae*. These overlaps of
217 *Gruiformes* with other bird clades persist when allometry is removed from shape, but in
218 addition, *Aequorlitornithes* cannot be distinguished from *Palaeognathae* anymore, as
219 indicated by the *PCA* results (Fig. 2 A, B). The overlap between clades increases with the
220 exclusion of species with flat vomers and non-adult semaphoronts (Supplementary Data S4:
221 Table S3, S4).

222 For the original dataset (A) with allometry included, the *DA* identifies all species
223 correctly as *Palaeognathae* or *Neognathae*. The error of false identification increases to 2.6%
224 if the data are *jackknifed*. When allometry is removed, the error increases to 13.2% before

225 and 36.8% after **jackknife** resampling. In the former case, the misidentifications are restricted
226 to neognath birds, which are wrongly classified as **Palaeognathae**, while **jackknifing** leads to
227 identification errors in both groups. For the five-group comparison, all species of dataset (A)
228 are correctly identified, when allometry is still present. The error is 18.4% after **jackknife**
229 resampling, showing minor mismatches in all clades. Excluding allometry, the error increases
230 to 10.5% before and 47.4% after **jackknifing**. While in the former case, a few
231 **Aequorlitorornithes** (2) and **Inopinaves** (1) species are wrongly identified as **Palaeognathae**
232 (Fig. 2 C, D), **Palaeognathae** cannot be separated from the neognath subclades anymore after
233 resampling. The exclusion of species with flat vomers and non-adult semaphoronts leads to
234 an increase of error (**Supplementary Data S4: Table S3-S6**).

235 The *pFDA* found 15.8% of **incorrect identifications** when **Palaeognathae** are
236 compared with neognaths in the original dataset (A). This error increases to 31.6% if shape is
237 corrected for allometry. In both cases, error is primarily based on the **incorrect identification**
238 of palaeognath specimens as neognaths. When **Palaeognathae** are compared with neognath
239 subclades, the error of correct identification is 10.5% before and 26.3% after allometry is
240 removed from the data. For the allometric data, the **misidentifications** result from the overlap
241 between **Paleognathae**, **Aequorlitorornithes** and **Gruiformes**. The misidentifications between
242 these three groups are increased when shape is corrected for allometry, while **Inopinaves** are
243 in part also wrongly identified as **Palaeognathae**. The exclusion of species with a flat vomer
244 and/or non-adult semaphoronts usually causes a decrease of false identifications. However,
245 the non-allometric dataset shows an increase in error for the two-group comparison, when
246 species with flat vomers are excluded, and for the five-group comparison, when only adult
247 semaphoronts are taken into account (Fig. 2 E, F). Nevertheless, for all four datasets, the error
248 of correct identification is significantly higher for non-allometric vomer shapes (Fig 3A,
249 **Supplementary Data S4: Table S3-S6**).

250

251 **Discussion**

252 The skull of crown birds possesses a complex kinetic system that includes a mobilized
253 quadrate, the zygomatic arch (= jugal bar) and the pterygoid-palatine complex (PPC) that
254 allows for the simultaneous, but restricted motion of both jaws (Bock 1964; Zusi 1984).
255 According to Zusi (1984), the kinetic system can be differentiated into three main types: (1)
256 **prokinesis** describes the rotation of the whole beak around the nasal-frontal hinge; (2)
257 **amphikinesis** is derived from prokinesis, including the rotation of the beak around the nasal-
258 frontal hinge plus an additional flexion of the anterior portion of the beak; **and** (3)
259 **rhynchokinesis**, **which in contrast** includes a simple flexion of the beak around one or several
260 bending zones rostral to the nasal-frontal suture, lacking a true hinge. Depending on the
261 position of the bending zones, rhynchokinesis can be further differentiated into five subtypes
262 **(Zusi 1984)**. Most palaeognath birds possess central rhynchokinesis, while neognaths have
263 realized all types of cranial kinesis (Zusi 1984), including some taxa with akinetic skulls
264 (Reid 1835; Sims 1955; Degrange et al. 2010). In the past, several authors (Hofer 1954;
265 Simonetta 1960; Bock 1963) suggested a close relationship between the morphology of the
266 PPC and type of cranial kinesis. However, Gussekloo et al. (2001) demonstrated that all types
267 of kinesis present in crown birds have similar movements of the quadrate, zygomatic arch
268 and PPC. **Palaeognathae** and **Neognathae** only differ in the magnitude of kinetic movements
269 in that **Palaeognathae** have slightly more restricted movement due to their rigid palate
270 missing a movable joint between the pterygoid and palatine (Gussekloo et al. 2005).

271 Thus, although the **results of geometric morphometric analysis** of the vomer shape by
272 Hu et al. (2019) **imply at first glance** a distinct separation between **Palaeognathae** and
273 **Neognathae**, this separation does not necessarily reflect their conclusions regarding the
274 evolution of cranial kinesis in crown birds, **i.e., that cranial kinesis represents an innovation**

275 of *Neognathae*. As indicated by the *PCA*, *Palaeognathae* occupy an enormous vomeral
276 morphospace (Hu et al. 2019), which mirrors their generally large palatal disparity (see
277 McDowell 1948) and partly overlaps with *Gruiformes* and *Aequorlithornithes*. In all cases
278 tested, however, the exclusion of allometric shape variation generally increases the error of
279 misidentification between all groups (Fig. 3A; Supplementary Data S4: Table S7), indicating
280 that the taxonomic distinctions of shape found by Hu et al. (2019) are at least partly an
281 artefact of size. This primarily concerns PC2, which according to Hu et al. (2019) separates
282 *Palaeognathae* from *Neognathae*, but also contains the major part of allometric information.
283 According to shape variation explained by PC2, larger birds tend to evolve vomers that are
284 more dorsoventrally compressed. Only members of the *Galloanserae* could be still identified
285 with a high amount of certainty when allometry is excluded.

286 Thus, our finding supports previous studies that demonstrated a relevant impact of
287 allometry on skull shape evolution in birds (Klingenberg & Marugán-Lobón 2013; Bright et
288 al. 2016; Linde-Medina 2016; Tokita et al. 2016, Bright et al. 2019). By modifying the
289 dataset, it becomes further clear that both the homoplastic presence of flat vomers in
290 *Aequorlithornithes*, *Inopinaves*, *Galloanserae* (Dataset B) and ontogenetic variation (Dataset
291 C) affects the accuracy of taxonomic identification. In addition, *Palaeognathae* and
292 *Neognathae* do not differ in vomer size when compared to the head size (Fig. 3B).
293 Consequently, vomer shape is not practical for taxonomic identification and should not be
294 used as a proxy to infer the presence or absence of cranial kinesis in crown birds or their
295 stem. As the manifold shape diversity of crown bird's skulls is impaired by a tessellated
296 evolution with multiple convergent events (e.g., Zusi 1993; Felice & Goswami 2018), the use
297 of isolated elements for taxonomic identification and/or biomechanical implications should
298 be treated generally with some caution.

299 In fact, *DA* and *pFDA* frequently identified the troodontid *Sinovenator changii* and
300 avialan *Sapeornis chaoyangensis* as neognaths or neognath subclades when allometry is
301 excluded, while the original dataset implied a referral to **Palaeognathae** (see also Hu et al.
302 2019). However, the skull anatomy of both species indicates no cranial kinesis (Xu et al.
303 2002; Wang et al. 2017; Yin et al. 2018; Hu et al. 2020).

304 The origin and evolution of cranial kinesis in the stem line of birds is still not well
305 understood due to the rarity of complete three-dimensional skulls. However, skull material
306 from the ornithurines *Ichthyornis dispars* and *Hesperornis regalis* indicates a certain degree
307 of rynchokinesis (Bühler et al. 1988; Field et al. 2018) that might be comparable to that of
308 extant **Palaeognathae** or some **Aequorlithornithes**, but further shows that this functional
309 character was already present before the origin of the crown. Their kinesis is indicated by the
310 loss of the jugal-postorbital bar and the ectopterygoid (resulting in a loss of contact in the
311 jugal with the skull roof and the palate), the presence of a mobile bicondylar quadrate and a
312 mobile joint between quadrate and quadratojugal. Recently, Plateau & Foth (2020) speculated
313 that the peramorphic bone fusion in the braincase could be also related to cranial kinesis, in
314 which the fusion-induced immobility constrains a controlled kinetic dorsoventral flexion of
315 the avian beak during biting/picking. Based on these characters, most Mesozoic Avialae
316 (including *Sapeornis chaoyangensis*) still had akinetic skulls, although some Enantiornithes
317 possessing a reduced jugal-postorbital bar might have evolved primitive kinesis convergently
318 to Ornithurae (O'Connor & Chiappe 2011).

319 **Allometry describes the relationship between size and shape, which is one of the key**
320 **concepts in biology to explain variation of shape in organisms (Klingenberg 1998), and is**
321 **crucial for studying taxonomy, ontogeny and functional morphology. Investigating the effect**
322 **of allometry on the vomer shape in crown birds with help of multiple multivariate statistical**
323 **methods, indicates that this bone is not a good proxy for taxonomy. Shape differences**

324 between Palaeognathae and Neognathae are clearly affected by size and can neither be used
325 to differentiate between different types of cranial kinesis nor to explain the evolution of
326 cranial kinesis within crown birds. In contrast, the evolution of cranial kinesis in birds needs
327 to be studied in context of the whole pterygoid-palatine complex and its contacts with the
328 braincase and quadrate-zygomatic arch.

329

330 **Acknowledgements**

331 We thank Walter Joyce Roland Sookias and Sergio Martínez Nebreda for their critical
332 comments on previous versions of the manuscript. The Swiss National Science Foundation is
333 thanked for its financial support (PZ00P2_174040 to C.F.).

334

335 **Additional information**

336 **Funding**

337 This study was funded by the Swiss National Science Foundation (PZ00P2_174040).

338

339 **Conflict of interest disclosure**

340 The authors of this article declare that they have no financial conflict of interest with the
341 content of this article. None of the authors is a *PCIPaleo* recommender.

342

343 **Author Approvals**

344 All authors have seen and approved the manuscript. The manuscript has not been accepted or
345 published elsewhere.

346

347 **Author contributions**

348 O.P. and C.F. designed the research project and analysed the data; and O.P. and C.F. wrote
349 the paper and prepared all figures.

350

351 **Data availability**

352 The 3D models and landmarks data of Hu et al. (2019) are available at Figshare (DOI:
353 <https://doi.org/10.6084/m9.figshare.7769279.v2>).

354

355 **Supplementary information**

- 356 • Data S1: Phylogenetic trees used for *pFDA*.
- 357 • Data S2: PCA results of all dataset before and after correction for allometry.
- 358 • Data S3: PCA plots of Dataset B-D before and after correction for allometry.
- 359 • Data S4: Results of npMANOVA, DA and pFDA.
- 360 • Data S5: R Code including all statistical analyses.

361

362 **References**

363 Adams DC, Otárola-Castillo E. 2013. *geomorph*: an R package for the collection and analysis
364 of geometric morphometric shape data. *Methods in Ecology and Evolution* 4:393–399.

365 Anderson MJ. 2001. A new method for non-parametric multivariate analysis of variance.
366 *Austral Ecology* 26:32–46.

367 Bellairs ADA, Jenkin CR. 1960. The skeleton of birds. In: Marshall AJ ed. *Biology and*
368 *Comparative Physiology of Birds, Vol. 1*. New York: Academic Press, 241–300.

369 Blomberg SP, Garland TJ, Ives AR. 2003. Testing for phylogenetic signal in comparative
370 data: behavioral traits are more labile. *Evolution* 57:717–745.

371 Bock WJ. 1963. The cranial evidence for ratite affinities. *Proceedings of the 13th*
372 *International Ornithological Congress* 1:39–54.

373 Bock WJ. 1964. Kinetics of the avian skull. *Journal of Morphology* 114:1–42.

374 Bridge ES, Jones AW, Baker AJ. 2005. A phylogenetic framework for the terns (Sternini)
375 inferred from mtDNA sequences: implications for taxonomy and plumage evolution.
376 *Molecular Phylogenetics and Evolution* 35:459–469.

377 Bright JA, Marugán-Lobón J, Cobb SN, Rayfield J. 2016. The shapes of bird beaks are highly
378 controlled by nondietary factors. *Proceedings of the National Academy of Sciences,*
379 *U.S.A.* 113:5352–5357.

380 Bright JA, Marugán-Lobón J, Rayfield J, Cobb SN. 2019. The multifactorial nature of beak
381 and skull shape evolution in parrots and cockatoos (Psittaciformes). *BMC Evolutionary*
382 *Biology* 19:1–9.

383 Bühler P, Martin LD, Witmer LM. 1988. Cranial kinesis in the Late Cretaceous birds
384 *Hesperornis* and *Paraesperornis*. *The Auk* 105:111–122.

385 Degrange F, Tambussi C, Moreno K, Witmer L, Wroe S. 2010. Mechanical analysis of
386 feeding behavior in the extinct “Terror Bird” *Andalgalornis steulleti* (Gruiformes:
387 Phorusrhacidae). *PLoS ONE* 5:e11856.

388 Felice RN, Goswami A. 2018. Developmental origins of mosaic evolution in the avian
389 cranium. *Proceedings of the National Academy of Sciences, U.S.A.* 115:555–560.

390 Field DJ, Hanson M, Burnham DA, Wilson LE, Super K, Ehret D, Ebersole JA, Bhullar B-
391 AS. 2018. Complete *Ichthyornis* skull illuminates mosaic assembly of the avian head.
392 *Nature* 557:96–100.

393 Goodall C. 1991. Procrustes methods in the statistical analysis of shape. *Journal of the Royal*
394 *Statistical Society: Series B (Methodological)* 53:285–321.

395 Gussekloo SWS, Bout RG. 2005. The kinematics of feeding and drinking in palaeognathous
396 birds in relation to cranial morphology. *The Journal of Experimental Biology* 208:3395–
397 3407.

398 Gussekloo SWS, Vosselman MG, Bout RG. 2001. Three-dimensional kinematics of skeletal
399 elements in avian prokinetic and rhynchokinetic skull determined by roentgen
400 stereophotogrammetrics. *The Journal of Experimental Biology* 204:1735–1744.

401 Hackett SJ, Kimball RT, Reddy S, Browie RCK, Braun EL, Chojnowski JL, Cox A, Han K,
402 Harshman J, Huddleston CJ, Marks BD, Miglia KJ, Moore WS, Sheldon FH, Steadman
403 DW, Witt CC, Yuri T. 2008. A phylogenomic study of birds reveals their evolutionary
404 history. *Science* 320:1763–1768.

405 Hammer O, Harper DAT. 2006. *Paleontological Data Analysis*. Malden: Blackwell
406 Publishing, 351 pp.

407 Hammer O, Harper DAT, Ryan PD. 2001. PAST: paleontological statistics software package
408 for education and data analysis. *Palaeontologia Electronica* 4:1–9.

409 Hammer O. 2020. *PAST Paleontological Statistics v.4.03. Reference Manual*. Oslo:
410 University of Oslo, 283 pp.

411 Hofer H. 1954. Neuere Untersuchungen zur Kopfmorphologie der Vögel. *Acta XI Congressus*
412 *Internationalis Ornithologici*:104–137.

413 Holdaway RN, Jacomb C. 2000. Rapid extinction of the moas (Aves: Dinornithiformes):
414 model, test, and implications. *Science* 287:2250–2254.

415 Hu H, O'Connor J, McDonald P, Wroe S. 2020. Cranial osteology of the Early Cretaceous
416 *Sapeornis chaoyangensis* (Aves: Pygostylia). *Cretaceous Research* 113:104496.

417 Hu H, Sansalone G, Wroe S, McDonald PG, O'Connor JK, Li Z, Xu X, Zhou Z. 2019.
418 Evolution of the vomer and its implications for cranial kinesis in Paraves. *Proceedings*
419 *of the National Academy of Sciences, U.S.A.* 116:19571–19578.

420 Huxley TH. 1867. On the classification of birds; and on the taxonomic value of the
421 modifications of certain cranial bones observable in the class. *Proceedings of the*
422 *Zoological Society of London* 27:415–472.

- 423 Jetz W, Thomas GH, Joy JB, Hartmann K, Mooers AO. 2012. The global diversity of birds in
424 space and time. *Nature* 491:444–448.
- 425 Jetz W, Thomas GH, Joy JB, Redding DW, Hartmann K, Mooers AO. 2014. Global
426 distribution and conservation of evolutionary distinctness in birds. *Current Biology*
427 24:1–12.
- 428 Klingenberg CP. 1998. Heterochrony and allometry: the analysis of evolutionary change in
429 ontogeny. *Biological Reviews* 73:79–123.
- 430 Klingenberg CP, Marugán-Lobón J. 2013. Evolutionary covariation in geometric
431 morphometric data: analyzing integration, modularity, and allometry in phylogenetic
432 context. *Systematic Biology* 62:591–610.
- 433 Krajewski C, Sipiorski JT, Anderson FE. 2010. Complete mitochondrial genome sequences
434 and the phylogeny of cranes (Gruiformes: Gruidae). *The Auk* 127:440–452.
- 435 Linde-Medina M. 2016. Testing the cranial evolutionary allometric “rule” in Galliformes.
436 *Journal of Evolutionary Biology* 29:1873–1878.
- 437 Mayr G. 2017. *Avian evolution*. Chichester: John Wiley, 293 pp.
- 438 McDowell S. 1948. The bony palate of birds. Part I. The Palaeognathae. *The Auk* 65:520–
439 549.
- 440 Mitchell K, Llamas B, Soubrier J, Rawlence N, Worthy T, Wood J, Lee M, Cooper A. 2014.
441 Ancient DNA reveals elephant birds and kiwi are sister taxa and clarifies ratite bird
442 evolution. *Science* 344:898–900.
- 443 Motani R, Schmitz L. 2011. Phylogenetic versus functional signals in the evolution of form-
444 function relationships in terrestrial vision. *Evolution* 65:2245–2257.
- 445 O’Connor JK, Chiappe LM. 2011. A revision of enantiornithine (Aves: Ornithothoraces)
446 skull morphology. *Journal of Systematic Palaeontology* 9:135–157.
- 447 Plateau O, Foth C. 2020. Birds have peramorphic skulls, too: anatomical network analyses

448 reveal oppositional heterochronies in avian skull evolution. *Communications Biology* 3.
449 R Development Core Team. 2011. *R: a language and environment for statistical computing*.
450 <http://www.r-project.org>.
451 Rauhut OWM, Tischlinger H, Foth C. 2019. A non-archaeopterygid avialan theropod from
452 the Late Jurassic of southern Germany. *eLife* 8:e43789.
453 Reid J. 1835. Anatomical description of the Patagonian penguin. *Proceedings of the*
454 *Zoological Society of London* 3:132–148.
455 Revell LJ. 2012. *phytools*: an R package for phylogenetic comparative biology (and other
456 things). *Methods in Ecology and Evolution* 3:217–223.
457 Schmitz L, Motani R. 2011. Nocturnality in dinosaurs inferred from scleral ring and orbit
458 morphology. *Science* 332:705–708.
459 Simonetta A. 1960. On the mechanical implications of the avian skull and their bearing on
460 the evolution and classification of birds. *The Quarterly Review of Biology* 35:206–220.
461 Sims S. 1955. The morphology of the head of the hawfinch (*Coccothraustes coccothraustes*).
462 *Bulletin of the British Museum* 2:371–393.
463 Tokita M, Yano W, James H, Abzhanov A. 2016. Cranial shape evolution in adaptive
464 radiations of birds: comparative morphometrics of Darwin’s finches and Hawaiian
465 honeycreepers. *Philosophical Transactions of the Royal Society B* 372:20150481.
466 Turvey ST, Holdaway RN. 2005. Postnatal ontogeny, population structure, and extinction of
467 the giant moa *Dinornis*. *Journal of Morphology* 265:70–86.
468 Wang Y, Hu H, O’Connor JK, Wang M, Xu X, Zhou Z, Wang X, Zheng X. 2017. A
469 previously undescribed specimen reveals new information on the dentition of *Sapeornis*
470 *chaoyangensis*. *Cretaceous Research* 74:1–10
471 Xu X, Norell MA, Wang X, Makovicky PJ, Wu X. 2002. A basal troodontid from the Early
472 Cretaceous of China. *Nature* 415:780–784.

473 Yin Y, Pei R, Zhou C. 2018. Cranial morphology of *Sinovenator changii* (Theropoda:
474 Troodontidae) on the new material from the Yixian Formation of western Liaoning,
475 China. *PeerJ* 6:e4977.

476 **Zelditch ML, Swiderski DL, Sheets HD. 2012. *Geometric morphometrics for biologists: a***
477 ***primer*. Amsterdam: Elsevier Academic Press, 488 pp.**

478 Zusi RL. 1984. A functional and evolutionary analysis of rynchokinesis in birds.
479 *Smithsonian Contributions to Zoology* 395:1-40.

480 Zusi RL. 1993. Patterns of diversity in the avian skull. In: Hanken J, Hall BK eds. *The skull*.
481 *Vol. 2. Patterns of structural and systematic diversity*. Chicago: University of Chicago
482 Press, 391–437.

483

484 **Figure legends**

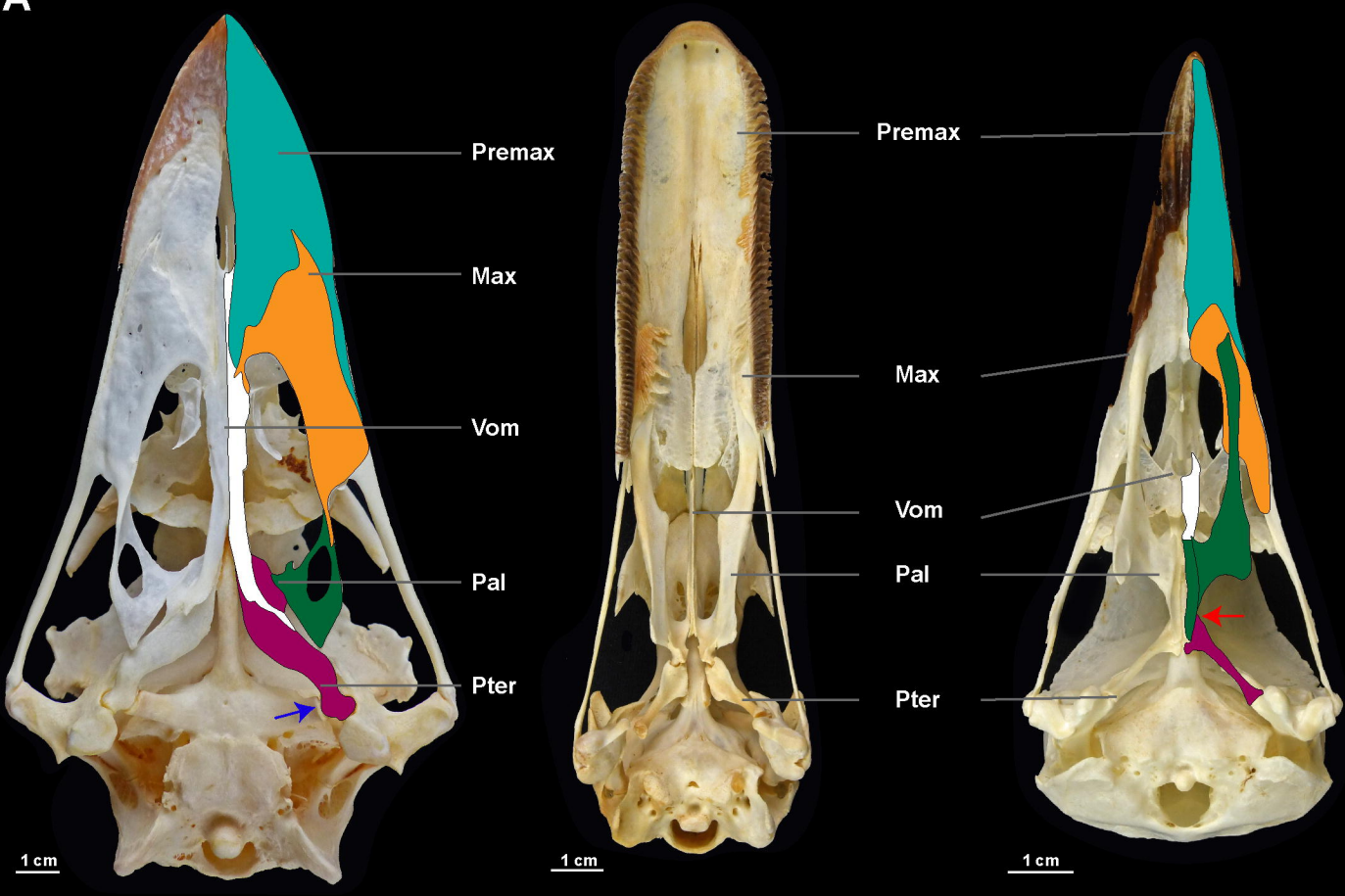
485 **Fig. 1. Anatomical organization of the pterygoid-palatine complex (PPC) and shape**
486 **variability of the vomer in palaeognath and neognath birds. (A)** Palates of *Dromaius*
487 *novaehollandia* (left), *Cygnus olor* (middle) and *Corvus corax* (right) in ventral view (all
488 specimens form the Natural History Museum of Fribourg/University of Fribourg). **For**
489 ***Dromaius novaehollandiae* and *Corvus corax* the main organization of palate morphology is**
490 **highlighted in a coloured scheme. The blue arrow in *Dromaius novaehollandiae* indicates the**
491 **contact between the basipterygoid process and the pterygoid. The red arrow in *Corvus corax***
492 **indicates the mobile joint between pterygoid and palatine. (B)** 3D models of the vomer of
493 *Dinornis robustus*, *Anas crecca* and *Strepera graculina* in lateral view (left) and anterior
494 view (right) from (not at scale) (3D models from Hu et al. 2019). **Abbreviations:** Max,
495 Maxillary; Pal, Palatine; Premax, Premaxillary; Pter, Pterygoid; Vom, Vomer.

496

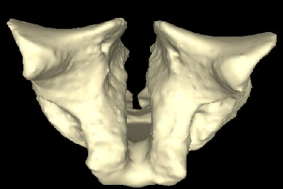
497 **Fig. 2. Differences between allometric and non-allometric morphospaces of the vomer**
498 **(Dataset A) in palaeognath and neognath birds. (A) PCA (*Principal Component Analysis*)**
499 results of allometric data. **(B) PCA** results of non-allometric data. **(C) DA (*Discriminant***
500 ***Analysis*)** results of allometric data. **(D) DA** results of non-allometric data. **(E) *pFDA***
501 ***(phylogenetic Flexible Discriminant Analysis)*** results of allometric data. **(F) *pFDA*** results of
502 non-allometric data. Centroid sizes (Csize) are indicated by the size of the symbols. All
503 silhouettes are taken from <http://www.phylopic.org/>.

504

505 **Fig. 3. Errors of correct taxonomic identification for all comparisons of Dataset A-D.**
506 **(A)** Two-group identification (Palaeognathae and Neognathae) before (red) and after (green)
507 correction for allometry. *DA*, Discriminant analysis; *DA*JK*, Discriminant Analysis with
508 jackknife resampling; *pFDA*, phylogenetic Flexible Discriminant Analysis. **(B)** Five-group
509 identification (Palaeognathae, Aequirornithes, Galloanserae, Gruiformes and Inopinaves).
510 **(C)** *OLS* regression (black line) between log-transformed skull box volume and log-
511 transformed centroid size of the vomer. Grey shadow marks the area of the 95% confidence
512 interval.

A*Dromaius novaehollandiae**Cygnus olor**Corvus corax*

Premax
 Max
 Vom
 Pal
 Pter

B*Dinornis robustus**Anas crecca**Strepera graculina*

Dorsal
Anterior

Dorsal
Lateral

